

Phonon Dispersion of Ice under Pressure

Th. Strässle,* A. M. Saitta, and S. Klotz

Physique des Milieux Condensés, Université Pierre et Marie Curie B77, 75252 Paris, France

M. Braden

II. Physikalisches Institut, Universität zu Köln, 50937 Köln, Germany

Laboratoire Léon Brillouin, CE Saclay, 91191 Gif-sur-Yvette, France

(Received 2 September 2004; published 23 November 2004)

We report measurements of the phonon dispersion of ice *Ih* under hydrostatic pressure up to 0.5 GPa, at 140 K, using inelastic neutron scattering. They reveal a pronounced softening of various low-energy modes, in particular, those of the transverse acoustic phonon branch in the [100] direction and polarization in the hexagonal plane. We demonstrate with the aid of a lattice dynamical model that these anomalous features in the phonon dispersion are at the origin of the negative thermal expansion (NTE) coefficient in ice below 60 K. Moreover, extrapolation to higher pressures shows that the mode frequencies responsible for the NTE approach zero at ~ 2.5 GPa, which explains the known pressure-induced amorphization (PIA) in ice. These results give the first clear experimental evidence that PIA in ice is due to a lattice instability, i.e., mechanical melting.

DOI: 10.1103/PhysRevLett.93.225901

PACS numbers: 65.60.+a, 62.50.+p, 78.70.Nx

Among the thirteen known crystalline ice phases, ordinary ice (ice *Ih*) exhibits several unusual features. First, ice *Ih* shows a negative thermal expansion (NTE) at temperatures below ~ 60 K and ambient pressure ([1], and references therein). Second, at temperatures below 130 K, ice *Ih* undergoes a transition to an amorphous phase when compressed above ~ 1.5 GPa [2]. NTE is commonly ascribed to a softening of transverse acoustic (TA) phonon branches with increasing pressure as, e.g., often found in tetrahedrally coordinated compounds [3–5]. Pressure-induced amorphization (PIA) was first observed by Brixner in $\text{Gd}_2(\text{MoO}_4)_3$ [6]. Broader interest in PIA was found later after the discovery by Mishima *et al.* that ordinary ice *Ih* also undergoes a transformation to an amorphous phase [2]. Subsequently, PIA was found in a wide group of compounds ([7], and references therein) including some minerals of geophysical importance, notably SiO_2 . Despite the growing interest in this phenomenon, the microscopic mechanism underlying PIA has remained obscure. Broadly speaking, three different mechanisms have been proposed ([7], and references therein). First, amorphization was proposed to be associated with thermodynamical melting. Many of the materials undergoing PIA exhibit melting lines with negative slopes, which, if extrapolated into the metastable domain of other crystalline phases at low temperatures, correspond approximately to pressures where PIA was indeed observed (see, e.g., [2] for ice). Second, lattice instabilities due to softening of TA phonon branches were proposed for being responsible for PIA, commonly referred to as “mechanical melting” (see, e.g., [8–10] for ice). Third, steric constraints were proposed leading to an amorphization [11].

Support for the scenario of mechanical melting has come mainly from molecular dynamics (MD) simulations [8,9,12–14] and other theoretical studies [10,15–

18]. These indicate that lattice instabilities occur at approximately those pressures where PIA is observed experimentally. However, it was also argued that a transition into a truly amorphous state has probably never been directly observed in MD calculations [19]. Empirically one finds that many NTE materials undergo amorphization under pressure, thus supporting the concept of phonon softening being involved in the amorphization process [6,7,11,20]. Experimental studies on the microscopic origin of PIA are, however, extremely scarce due to the difficulty to observe complete phonon dispersion curves under pressure. In the case of α quartz, Brillouin spectroscopy [21] revealed, indeed, a zone-center lattice instability at an extrapolated pressure somewhat higher than where amorphization is observed experimentally but in agreement with MD calculations [15]. Other theoretical studies [16] support the occurrence of a zone-boundary lattice instability possibly associated with the transition to another crystalline phase of α quartz induced by pressure prior to amorphization [22]. As for ice, ultrasonic measurements on polycrystalline samples detected a softening of the shear velocities prior to the amorphization, which was interpreted as a precursor effect of a lattice instability [23].

The question regarding how far phonons are involved in PIA and their relation to NTE hence remains unclear and can be elucidated only by a better understanding of the behavior of the phonons under pressure. As opposed to Brillouin and ultrasonic studies, neutron spectroscopy gives access to the entire dispersion curves and thus is able to differentiate between zone-center and zone-boundary anomalies in the lattice dynamics. Ice *Ih* represents an ideal system for the study of the microscopic mechanism of PIA since it exhibits amorphization at moderately high pressures.

We have applied inelastic neutron scattering (INS) using several single crystals of deuterated ice *Ih* of 0.5–1 cm³ volume and excellent quality (mosaic spread <0.5°). Strictly hydrostatic pressure up to 0.55 GPa was applied by use of a gas pressure cell and fluid nitrogen as a pressure medium [24]. The temperature was kept constant at 140 K in a standard He cryostat. All measurements were carried out in a fixed final energy configuration ($E_F = 3.55$ THz) on the triple-axis spectrometer 1T1 of the Laboratoire Léon Brillouin in Saclay (France). The dispersion was measured along the high symmetry directions of the hexagonal crystal (space group $P63/mmc$, $Z = 4$) close to ambient pressure at $P = 0.05$ GPa, at a maximum pressure of 0.5 GPa, and at three intermediate pressures, giving a total of 320 phonon frequencies.

Figure 1 shows representative neutron spectra of the lowest basal TA phonon in ice *Ih* at pressures of $P = 0.05$ and 0.5 GPa. Strong softening is observed for phonons with both the propagation direction and the polarization in the basal plane. However, whereas phonon frequencies at the zone-boundary M point decrease considerably, the softening of the corresponding phonon at the K point is close to zero. The symbols in Fig. 2 show the full phonon dispersion measured at $P = 0.05$ and 0.5 GPa. Our low pressure data are in good agreement with the only other available INS study on the complete phonon dispersion of ice measured at ambient pressure by Renker [25,26], except for one aspect: our data reveal a clear splitting of the two TA branches in the Γ - M direction, a detail which is also visible in earlier data [27] and which is confirmed by our *ab initio* calculations discussed further below.

In order to extract values of the elastic and thermal properties from our phonon measurements, we developed a lattice dynamical model similar to the one introduced by Renker [25,26] and fitted to it the measured data at various pressures (Fig. 2, top). For this purpose the pressure dependence of the Raman active mode at 7 THz determined by Garg [28] was included in the neutron data set. The simple Born–von Kármán (BvK) model

considers the D₂O water molecules as particles of mass 20 interacting via nearest neighbor forces described by only six force constants. They describe longitudinal, transverse, and angular forces towards basal and axial neighbors, respectively [29]. Fits to the data taken at $P = 0.05, 0.2, 0.25, 0.35,$ and 0.5 GPa show a linear dependence in both the six force constants as well as in the elastic constants yielded from the model. Relative changes in the elastic constants between ambient pressure and $P = 0.5$ GPa may be compared with earlier Brillouin studies by Gagnon *et al.* [30], carried out at 237 K (shown in brackets): $\Delta c_{11}/c_{11} = +12\%(+12\%)$, $\Delta c_{33}/c_{33} = +13\%(+12\%)$, $\Delta c_{44}/c_{44} = -4\%(-5\%)$, $\Delta c_{66}/c_{66} = -17\%(-11\%)$, $\Delta c_{13}/c_{13} = +37\%(+36\%)$. Given the very good agreement of this model with the measured phonon frequencies (mean square deviation less than 0.1 THz) as well as with the elastic constants under pressure, we conclude that this BvK approach contains the essential physics of the behavior of the low-energy lattice modes of ice under pressure.

The lattice dynamical model now allows us to extract various thermal properties of ice *Ih* at elevated pressures. Mode frequencies were sampled on a grid of $50 \times 50 \times 50$ equidistantly distributed q points in an irreducible wedge of the Brillouin zone (BZ). Figure 3 shows the resulting phonon densities of states (PDOS) at $P = 0.05$ and 0.5 GPa. The contribution from TA phonon branches is clearly visible by the anomalous negative shift of modes below ~ 120 K (2.5 THz), whereas features at higher energies, arising from the longitudinal acoustic and optical branches, show the opposite tendency.

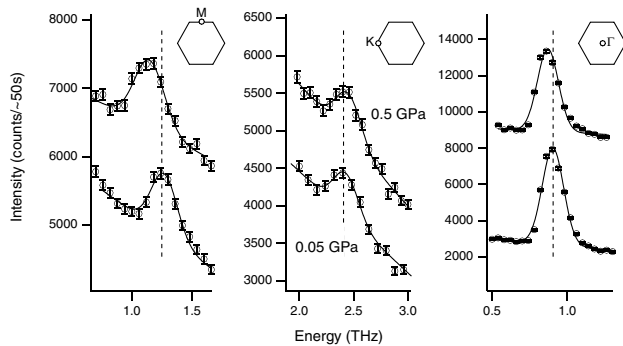


FIG. 1. Neutron spectra of the lowest basal TA phonon in ice *Ih* ($T = 140$ K) at $P = 0.05$ and 0.5 GPa (lower and upper curves, respectively) [measured at $(-1 + q, 2, 0)$ with $q = 1/2$, at $(-1 + 2q, 2 - q, 0)$ with $q = 1/3$ and at $(-1 + 2q, 2 - q, 0)$ with $q = 0.1$, respectively].

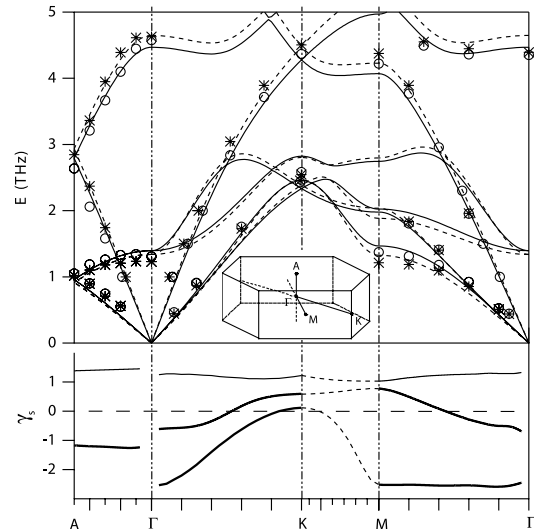


FIG. 2. Top: Measured phonon dispersion of ice *Ih* ($T = 140$ K) at $P = 0.05$ GPa (circles) and $P = 0.5$ GPa (stars). The solid and dashed lines are fits using the lattice dynamical model discussed in the text. Bottom: Mode Grüneisen parameters γ_s of the transverse and longitudinal acoustic branches (thick and thin lines, respectively) resulting from the evaluation of the model at $P = 0.05$ and 0.5 GPa.

Hence, qualitatively, NTE in ice *Ih* already becomes evident from the PDOS. Quantitative insight into the NTE can be gained by calculation of the overall Grüneisen parameter Γ and the linear thermal expansion coefficient α , given by

$$\Gamma = \sum_{k,s} \gamma_{ks} c_s(k), \quad \alpha = \frac{\Gamma C}{3BV}, \quad (1)$$

where $\gamma_{ks} = -\partial(\ln\omega_{ks})/\partial(\ln V)$ and $c_s(k) = \partial_T(\langle n_{ks} \rangle \hbar\omega_{ks})$ denote the mode Grüneisen parameters and mode specific heat capacities, respectively, and with ω_{ks} , n_{ks} , B , and V the phonon frequencies, thermal population factor, bulk modulus, and volume.

The inset of Fig. 3 shows that the dispersion-reconstructed value of α is in very good quantitative agreement [31] with the most accurate data from the literature ([1], and references therein, [32]). Our data thus provide unambiguously the lattice dynamical origin of the observed NTE in ordinary ice *Ih* and identify the responsible TA branches. The bottom part of Fig. 2 shows the mode Grüneisen parameters γ_s resulting from the model fits at $P = 0.05$ and 0.5 GPa [Eq. (1)]. Pronounced softening of the entire TA branch associated with the elastic constant c_{66} in the Γ - M direction (with mode Grüneisen parameters around -2.5) and softening of the respective branch close to the zone center in the Γ - K direction are observed. Further, in the Γ - A direction the two degenerate TA branches associated with c_{44} soften with a constant Grüneisen parameter of around -1 , while in the Γ - M and the Γ - K directions the respective TA branches show only negative values close to the zone center [33].

The linearity in the pressure dependence of both the elastic constants as well as the parameters of the lattice dynamical model up to 0.5 GPa allows for an extrapolation to higher pressures. We find that at $P_c \sim 2.5$ GPa corresponding to a relative volume reduction $\Delta V/V = -0.14$, the two TA branches responsible for NTE both

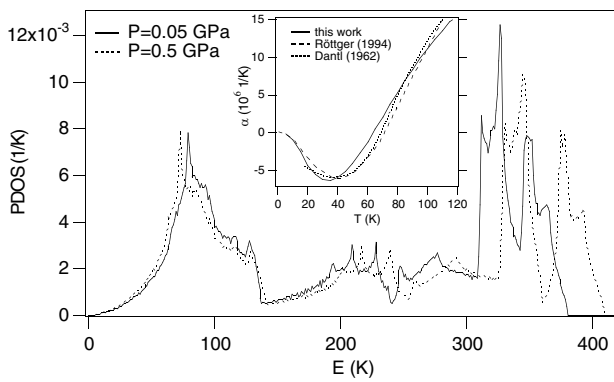


FIG. 3. Phonon density of states (PDOS) ($T = 140$ K) at $P = 0.05$ and 0.5 GPa. Inset: linear thermal expansion coefficient α of D_2O ice *Ih* reconstructed (solid line) from the measured phonon dispersion in comparison with literature data (dashed lines).

become flat near the zone center along Γ - M and Γ - K . This provides the essential link to the PIA in ice, since the complete softening of a substantial part or of a full acoustic phonon branch can be associated with PIA via a simultaneous freezing of a (infinite) set of wave vectors in the BZ [7,19]. In the present case, the flattening of the lower basal TA branches is equivalent to the elastic constant $c_{66} = (c_{11} - c_{12})/2$ approaching zero at P_c and corresponds to a violation of one of Born's stability criteria [34], which for hexagonal symmetry read

$$\begin{aligned} B_1 &:= c_{44} > 0, & B_2 &:= c_{11} - |c_{12}| > 0, \\ B_3 &:= (c_{11} + c_{12})c_{33} - 2c_{13}^2 > 0, \end{aligned} \quad (2)$$

where c_{ij} are the elastic constants defined from the stress-strain relation and which correspond to elastic constants determined from measurements of the sound velocity [16,17]. Figure 4 shows that B_2 as well as B_3 are almost simultaneously violated at ~ 2.5 GPa, whereas B_1 still holds.

In order to put the results obtained by the simple BvK model applied to pressures beyond 0.5 GPa on a firm ground, we also carried out *ab initio* calculations within the density-functional theory and density-functional perturbation theory frameworks, adopting a standard plane-wave/pseudopotential scheme within the Perdew-Burke-Ernzerhof gradient corrections approximation [35]. We determined the pressure-volume equation of state of proton-ordered ice *Ih*, and calculated its complete phonon dispersions at four different pressures up to about 4 GPa. Our calculations show up to 0.5 GPa a pressure-induced softening of the entire Γ - M TA branch, which is in remarkably good agreement with the experiments. More importantly, our calculations show evidence that the softening becomes complete at $\Delta V/V \sim -0.15$.

The above analysis of our results implies that the extrapolated critical pressure for two of the Born criteria being violated is about 1 GPa higher than the experimentally observed pressure where amorphization in ice *Ih* sets in. However, the simple linear extrapolation of the force constants is likely to overestimate P_c , since a nonlinear

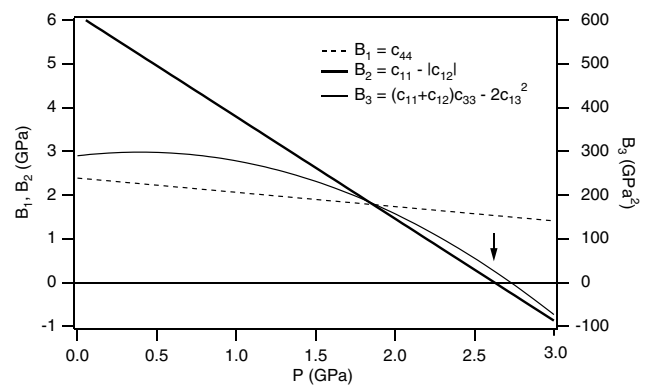


FIG. 4. Born's stability criteria as a function of pressure. B_2 and B_3 are almost simultaneously violated at $P_c \sim 2.5$ GPa.

behavior in the phonon frequencies is expected at pressures beyond $\sim 5\%$ of the bulk modulus [4,5]. Also, we emphasize the strong similarities between ice *Ih* and silica. In silica (α quartz) a violation of Born's criteria was estimated to ~ 39 GPa [21], whereas experimentally amorphization is found to start at ~ 22 GPa. We further note that mechanical melting, in the framework of Born's stability criteria, refers to the homogeneous limit and thus *per se* always defines an absolute upper limit for the crystalline structure to persist [12]. Strain fluctuations may lower the experimentally observed critical pressure for the lattice instability to set in heterogeneously.

While the present work constitutes the first experimental investigation on this issue, two previous theoretical studies have suggested that amorphization of ice is due to violation of Born's stability criteria. Based on classical MD calculations Tse *et al.* [8,9] have found that the amorphization in ice *Ih* is due to a violation of B_2 and B_3 [Eq. (2)]. Equally, recent *ab initio* calculations for ice XI (the ordered phase of ice *Ih*) have found B_2 being violated on the basis of the same theoretical approach as our *ab initio* calculations [10]. We note that a violation of one of Born's stability criteria solely indicates a transition to another phase, however, not necessarily to an amorphous one. On the other hand, our experimental data, as well as our *ab initio* calculations, show an almost dispersionless softening of the lower TA branch along the entire Γ - M direction and near the zone center along Γ - K (Fig. 2, bottom). This very fact suggests that, in the case of ice *Ih*, the lattice instability indeed leads to amorphization of the system via an almost simultaneous freezing of an infinite set of phonons with different q vectors due to drastically reduced bandwidths of the basal TA phonon branches [7,19].

This work was funded by the Swiss National Science Foundation (T.S., 81EZ-68588). Access to beam time at ISIS by R. J. Nelmes and J. S. Loveday and to the IDRIS French National Computational Facility (31387-CP9, 41387-CP9) is gratefully acknowledged. We are indebted to F. Méducin for cooperation at the early stage of this project and to S. Baroni and Ph. Pruzan for discussions.

*Electronic address: ts@pmc.jussieu.fr

- [1] K. Röttger, A. Endriss, J. Ihringer, S. Doyle, and W. F. Kuhs, *Acta Crystallogr. Sect. B* **50**, 644 (1994).
- [2] O. Mishima, L. D. Calvert, and E. Whalley, *Nature (London)* **310**, 393 (1984).
- [3] T. F. Smith and G. K. White, *J. Phys. C* **8**, 2031 (1975).
- [4] S. Klotz *et al.*, *Phys. Rev. Lett.* **79**, 1313 (1997).
- [5] S. Klotz, M. Braden, J. Kulda, P. Pavone, and B. Steininger, *Phys. Status Solidi B* **223**, 441 (2001).
- [6] L. H. Brixner, *Mater. Res. Bull.* **7**, 879 (1972).
- [7] S. M. Sharma and S. K. Sikka, *Prog. Mater. Sci.* **40**, 1 (1996).
- [8] J. S. Tse, *J. Chem. Phys.* **96**, 5482 (1992).
- [9] J. S. Tse *et al.*, *Nature (London)* **400**, 647 (1999).
- [10] K. Umemoto, R. M. Wentzcovitch, S. Baroni, and S. Gironcoli, *Phys. Rev. Lett.* **92**, 105502 (2004).
- [11] S. K. Sikka, *J. Phys. Condens. Matter* **16**, S1033 (2004).
- [12] D. Wolf, P. R. Okamoto, S. Yip, J. F. Lutsko, and M. Kluge, *J. Mater. Res.* **5**, 286 (1990).
- [13] S. L. Chaplot and S. K. Sikka, *Phys. Rev. B* **47**, 5710 (1993).
- [14] J. S. Tse and D. D. Klug, *Phys. Rev. Lett.* **67**, 3559 (1991).
- [15] N. Binggeli and J. R. Chelikowsky, *Phys. Rev. Lett.* **69**, 2220 (1992).
- [16] N. Binggeli, N. R. Keskar, and J. R. Chelikowsky, *Phys. Rev. B* **49**, 3075 (1994).
- [17] N. R. Keskar, J. R. Chelikowsky, and R. M. Wentzcovitch, *Phys. Rev. B* **50**, 9072 (1994).
- [18] D. W. Dean, R. M. Wentzcovitch, N. R. Keskar, J. R. Chelikowsky, and N. Binggeli, *Phys. Rev. B* **61**, 3303 (2000).
- [19] M. H. Cohen, J. Iniguez, and J. B. Neaton, *J. Non-Cryst. Solids* **307–310**, 602 (2002).
- [20] C. A. Perottoni and J. Jornada, *Science* **280**, 886 (1998).
- [21] E. Gregoryanz, R. J. Hemley, H. K. Mao, and P. Gillet, *Phys. Rev. Lett.* **84**, 3117 (2000).
- [22] K. J. Kingma, C. Meade, R. J. Hemley, H. K. Mao, and D. R. Veblen, *Science* **259**, 666 (1993).
- [23] E. L. Gromnitskaya, O. V. Stal'gorova, and V. V. Brazhkin, *Sov. Phys. JETP* **85**, 109 (1997).
- [24] The formation of nitrogen hydrates can be ruled out. We have performed separate neutron diffraction measurements (PEARL at ISIS, U.K.) on polycrystalline ice *Ih* at identical experimental conditions (140 K, 0.5 GPa) where even after 12 h no detectable amount of hydrates could be found.
- [25] B. Renker, *Phys. Lett.* **30A**, 493 (1969).
- [26] B. Renker, in *Physics and Chemistry of Ice*, edited by E. Whalley *et al.* (Royal Society of Canada, Ottawa, 1973), p. 82.
- [27] S. M. Bennington, J. M. J. Harris, and D. K. Ross, *Physica (Amsterdam)* **263–264B**, 396 (1999).
- [28] A. K. Garg, *Phys. Status Solidi A* **110**, 467 (1988).
- [29] The program GENAX was used [W. Reichardt (unpublished)]. The following parameters (dyn/cm) were found at $P = 0.05$ (0.5) GPa: $L_{\parallel} = 28\,256$ (33\,616), $T_{\parallel} = -1306$ (-2198), $\alpha_{\parallel} = 856$ (1119), $L_{\perp} = 20\,696$ (23\,277), $T_{\perp} = -1030$ (-1851), $\alpha_{\perp} = 815$ (1004).
- [30] R. E. Gagnon, H. Kiefte, M. J. Clouter, and E. Whalley, *J. Chem. Phys.* **89**, 4522 (1988).
- [31] We note that molecular solids commonly show well-separated translational and librational bands. Our lattice dynamical model cannot reproduce the librational bands. These start to be populated at $T \gtrsim 100$ K, which is why α shows deviations for $T \gtrsim 100$ K.
- [32] G. Dantl, *Z. Phys.* **166**, 115 (1962).
- [33] Details on the PDOS and γ_s will be published separately.
- [34] M. Born and K. Huang, *Dynamical Theory of Crystal Lattices* (Clarendon, Oxford, 1954).
- [35] S. Baroni, P. Giannozzi, and A. Testa, *Phys. Rev. Lett.* **58**, 1861 (1987), PWSCF code, www.pwscf.org.